

Magnetoresistance of a two-dimensional electron gas in a strong periodic potential

P. H. Beton, E. S. Alves, P. C. Main, L. Eaves, M. W. Dellow, M. Henini, and O. H. Hughes
Department of Physics, University of Nottingham, Nottingham NG7 2RD, United Kingdom

S. P. Beaumont and C. D. W. Wilkinson
Department of Electronic and Electrical Engineering, University of Glasgow, Glasgow G12 8QQ, United Kingdom
 (Received 20 August 1990)

We have investigated the magnetoresistance of a two-dimensional electron gas subjected to a periodic potential of variable amplitude. The periodic potential, of period 300 nm, is generated with use of a gate deposited over a layer of patterned resist, and its amplitude is controlled by the gate voltage. At low gate voltages, two series of oscillations periodic in inverse magnetic field are observed. One series, at low magnetic field, is due to the periodic potential and the other is the usual Shubnikov-de Haas oscillations. The application of a small gate voltage generates an increase in the amplitude of the low-field oscillations, followed by a quenching of these oscillations as the gate voltage is increased further. In addition, a low-field positive magnetoresistance is generated, becoming larger with increasing gate voltage. These effects are explained within a semi-classical model of electron transport. Also the Shubnikov-de Haas oscillations quench as the amplitude of the potential increases. This is explained in terms of a broadening of the Landau levels.

A series of oscillations periodic in $1/B$ (B is the magnetic field) have been observed in the magnetoresistance of a two-dimensional electron gas (2D EG) subjected to a weak one-dimensional^{1,2} or two-dimensional³ periodic potential. Several closely related explanations^{2,4-6} of the oscillations have been given, but work has so far focused on the effects of a weak applied potential. In this paper we discuss the dependence of the low-field oscillations on the amplitude of the potential. We emphasize the essentially classical nature of the oscillations which occur due to a resonant enhancement of the diffusivity and hence the conductivity σ_{yy} , in the direction parallel to the lines of constant potential. This results, for high-mobility samples, in an increase in the resistivity ρ_{xx} perpendicular to the lines. The enhancement occurs whenever $2R_c = (n + \frac{1}{4})a$, where $R_c = \hbar k_F / eB$ is the classical cyclotron radius at the Fermi momentum $\hbar k_F$, a is the period of the potential, and n is a positive integer.

Figure 1 shows a schematic diagram of the device. A "patterned gate" is formed on the surface of a modulation doped GaAs/(Al,Ga)As heterostructure in which a high-mobility 2D EG is embedded. Before lithography the mobility was $\sim 100 \text{ m}^2 \text{ V}^{-1} \text{ s}^{-1}$. The patterned gate comprises a layer of negative resist patterned by electron-beam lithography to give a series of lines. A Ti/Au layer is evaporated over this pattern to form a gate which is effective only where the metal adheres to the semiconduc-

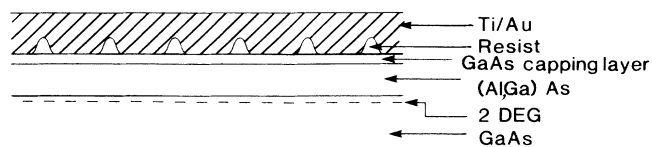


FIG. 1. Schematic diagram of the sample-fabrication process.

tor surface. Thus by biasing the gate we are able to generate a one-dimensional periodic potential in the plane of the 2D EG, the amplitude of which may be varied by varying the gate bias. The period of the potential is 300 nm, and the gate is deposited over a Hall bar of dimensions $5 \mu\text{m} \times 10 \mu\text{m}$, such that the current flows parallel to the longer direction and perpendicular to the lines of constant potential. We have measured the four terminal ac resistance of such a gated Hall bar as a function of magnetic field for various applied gate voltages at a temperature $T = 2 \text{ K}$. This data is shown in Fig. 2. When the gate voltage $V_g > -0.6 \text{ V}$, two series of oscillations periodic in $1/B$ are clearly visible. The low-field series of oscillations generated by the periodic potential terminates at

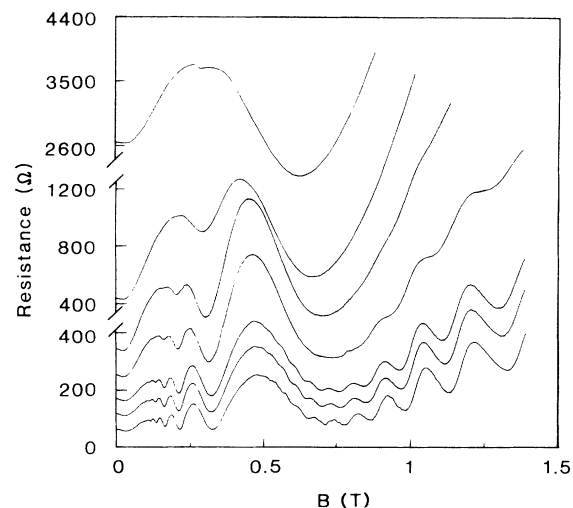


FIG. 2. Magnetoresistance at 2 K for a structure with $a = 300 \text{ nm}$. $V_g = -1.0$ (top), -0.8 , -0.6 , -0.5 , -0.3 (displaced by 100Ω), -0.2 (displaced by 50Ω), and 0 V (bottom).

$B \sim 0.7$ T. At higher fields Shubnikov-de Haas (SdH) oscillations are observed. As the negative gate bias is increased various effects are observed: (i) As expected the zero field resistance increases; (ii) a positive magnetoresistance is generated at magnetic fields below the onset of the low-field oscillations. The magnitude and field range of this magnetoresistance progressively increases with negative gate bias; (iii) the amplitude of the low-field oscillations initially increases but as the gate bias is made more negative these oscillations are quenched. The negative gate bias required to quench a particular maximum or minimum at a given magnetic field increases with magnetic field; (iv) the SdH oscillations are quenched by the application of a large negative gate bias.

The generation of the positive magnetoresistance and the suppression of the low-field oscillations are closely related and, as we argue below, can be explained by extending a theory due to Beenakker.⁴ The suppression of the SdH oscillations is due to a broadening of the Landau levels by the periodic potential.

As stated above the low-field oscillations are due to a resonant enhancement of the electron mobility parallel to the equipotentials when $2R_c = (n + \frac{1}{4})a$. This result was derived within a semiclassical framework.⁴ In the limit where eV_0 , the amplitude of the potential is small compared with the Fermi energy E_F . Typical electron trajectories at the Fermi energy for this weak limit are shown in Figs. 3(a) and 3(b). In both cases the ratio $\kappa \equiv eV_0/E_F$ is 0.01. The straight lines represent the maxima of the sinusoidal periodic potentials and the curves are the electron trajectories obtained by numerical integration of the semiclassical equation of motion. For the purposes of the simulation we took $E_F = 10$ meV above the minimum of the periodic potential. In Fig. 3(a) we have $2R_c = 6.25a$, a condition for the resonant enhancement of the electron mobility. The left-hand orbit is symmetric with respect to the periodic potential and hence is stationary, despite this resonant condition. However, all other orbits experience some drift, as shown for example by the right-hand orbit in Fig. 3(a). In Fig. 3(b), also in the limit $\kappa \ll 1$, $2R_c = 5.75a$ and *all* electron orbits are essentially stationary, regardless of the position of the orbit center. This corresponds to a minimum of the magnetoresistance oscillation. Insofar as all the orbits are stationary then there is no enhancement of σ_{yy} and $\rho_{xx} = \rho_0$, its value at $B = 0$.

In Figs. 3(c)–3(h) we plot electron trajectories for increasing V_0 . In Figs. 3(c) and 3(d), $\kappa = 0.05$. As well as the increased drift velocity in Fig. 3(c), which follows directly from the increase in potential since the drift velocity is proportional to the electric field generated by the periodic potential, there is also a slight visible distortion of the electron trajectories. In Fig. 3(d) the distortion has the effect of causing a previously stationary orbit to drift. This means that the minimum of the magnetoresistance oscillation no longer corresponds to a zero enhancement of σ_{yy} . The effect is even more pronounced in Figs. 3(e) and 3(f) where $\kappa = 0.09$. Here the drift induced by the distortion of the orbits in 3(f) is becoming comparable to the drift in 3(e)—the net effect is a considerable reduction in the contrast of the oscillations, largely due to an increase in resistance at the minima of the oscillations. Precisely

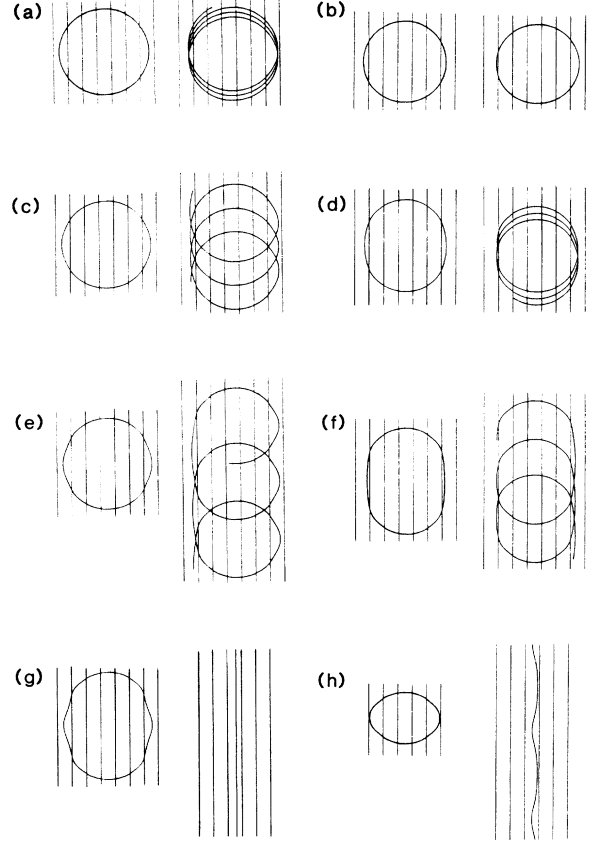


FIG. 3. Numerical simulations of the classical particle trajectories in a magnetic field and a periodic electric potential. The two left-hand columns are for $2R_c/a = 6.25$ and the two right-hand columns for $2R_c/a = 5.75$. The values of $\kappa \equiv eV_0/E_F$ are (a), (b) 0.01, (c), (d) 0.05, (e), (f) 0.09, and (g), (h) 0.15. The straight lines represent equipotential maxima.

the same effect occurs if, instead of increasing V_0 at constant B , we reduce B at constant V_0 . Thus the predictions of the numerical simulations are in good qualitative agreement with the experimental results shown in Fig. 2. Figures 3(g) and 3(h) illustrate the situation for $\kappa = 0.15$. Some orbits are still closed in both magnetic fields. However, there are now some orbits which are open. These orbits have a greatly enhanced drift, of order v_F rather than the somewhat smaller drift velocities of the closed orbits. Therefore, where they occur, the open orbits dominate ρ_{xx} . It is easy to show⁴ for $\omega_c \tau > 1$,

$$\frac{\Delta\rho_{xx}}{\rho_0} = \frac{\delta D_{yy}}{D_0} \omega_c^2 \tau^2 = \frac{\langle v_d^2 \rangle}{\frac{1}{2} v_F^2} \omega_c^2 \tau^2, \quad (1)$$

where $\delta D_{yy}/D_0$ is the relative diffusivity enhancement in the y direction, ρ_0 is the resistivity in zero magnetic field, ω_c is the classical cyclotron frequency, and τ is the scattering time. For the open orbits $\langle v_d^2 \rangle$, the mean-square drift velocity is $\sim v_F^2$ so Eq. (1) implies a magnetoresistance

$$\frac{\Delta\rho_{xx}}{\rho_0} \approx 2\omega_c^2 \tau^2 \frac{N_0}{N_T}, \quad (2)$$

where N_0 is the number of open electron orbits and N_T is the total number of electron orbits.

To calculate the fraction of electron orbits which are open we write down the classical electron Hamiltonian in the gauge $\mathbf{A} = (0, Bx, 0)$, for electrons at the Fermi energy E_F ,

$$\frac{p_x^2}{2m^*} + \frac{(p_y + eBx)^2}{2m^*} + eV_0 \cos\left(\frac{2\pi x}{a}\right) = E_F, \quad (3)$$

where p_x and p_y are the momentum components and m^* is the electron effective mass. E_F and p_y are constants of the motion. Each electron orbit can be represented by the position x_0 , where its motion is entirely along the y direction. Equation (3) then has the following solutions for $eV_0 \ll E_F$:

$$\frac{x_0 - x}{R_c} = 2 - \frac{eV_0}{2E_F} \left[\cos\left(\frac{2\pi x_0}{a}\right) + \cos\left(\frac{2\pi x}{a}\right) \right], \quad (4a)$$

$$\frac{x_0 - x}{R_c} = -2 + \frac{eV_0}{2E_F} \left[\cos\left(\frac{2\pi x_0}{a}\right) + \cos\left(\frac{2\pi x}{a}\right) \right], \quad (4b)$$

$$\frac{x_0 - x}{R_c} = \frac{eV_0}{2E_F} \left[\cos\left(\frac{2\pi x}{a}\right) - \cos\left(\frac{2\pi x_0}{a}\right) \right], \quad (4c)$$

$$\frac{x_0 - x}{R_c} = \frac{eV_0}{2E_F} \left[\cos\left(\frac{2\pi x_0}{a}\right) - \cos\left(\frac{2\pi x}{a}\right) \right]. \quad (4d)$$

The solutions 4(a) and 4(b) are closed orbits corresponding to motion in either the $+y$ or $-y$ direction at $x = x_0$. Equations 4(c) and 4(d) clearly have $x = x_0$ as one solution. However, there may be other solutions corresponding to open orbits where the electron starting from x_0 does not receive a sufficient increase of momentum from the Lorentz force to enable it to cross the first potential barrier it encounters. The condition that an electron starting from x_0 in the $+y$ direction has a *closed* orbit is

$$\frac{x_0 - x}{R_c} > \frac{eV_0}{2E_F} \left[\cos\left(\frac{2\pi x}{a}\right) - \cos\left(\frac{2\pi x_0}{a}\right) \right] \quad (5)$$

for all x such that $0 < x < x_0$. This can be written as

$$\frac{X_0 - X}{V} > \sin[\pi(X + X_0)] \sin[\pi(X_0 - X)], \quad (6)$$

where

$$V \equiv \left(\frac{R_c}{a}\right) \left(\frac{eV_0}{E_F}\right) = \frac{2V_0}{v_F a B},$$

$X = x/a$, and $X_0 = x_0/a$. The fraction of open orbits is a function only of V , i.e., for a given device, the ratio V_0/B . This fraction is plotted versus V in Fig. 4. The rapid onset of open orbits occurs at a threshold value $V = 1/\pi$. This has a very simple interpretation—it is the value of V_0/B for which the maximum electric force is equal to the magnetic force, i.e., $2\pi eV_0/a = eBv_F$.

Within the approximation of Eq. (2) we can calculate a classical magnetoresistance for any V_0 , a , v_F , and B . As an example, Fig. 5 shows magnetoresistance curves calculated for $E_F = 10$ meV, $\tau = 3 \times 10^{-12}$ s, $a = 300$ nm, and various values of V_0 . There is a strong similarity between these predictions and the data shown in Fig. 2. We associ-

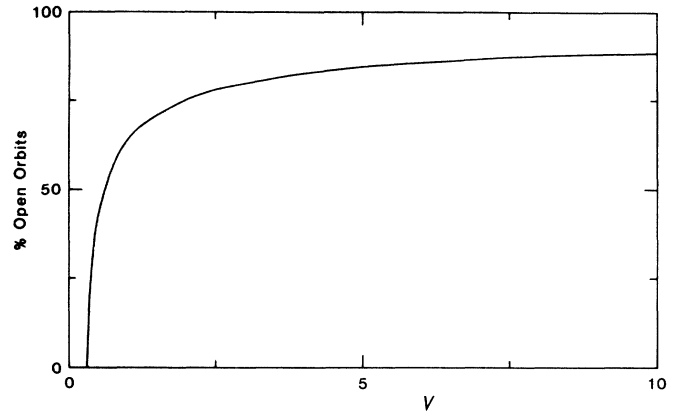


FIG. 4. The percentage of open orbits vs $V \equiv 2V_0/av_F B$.

ate the peak in the magnetoresistance with a rapid reduction in the number of open orbits. The values of B where the peak occurs for the data shown in Fig. 2 are listed in Table I together with the deduced values of V_0 . We predict, therefore, that the position of the peak in magnetic field should scale as $1/a$. Therefore, a smaller period leads, all things being equal, to a peak in magnetoresistance at a higher field. This is in agreement with our observation. At low B , $V \gg 1/\pi$ and there is a large proportion of open orbits and we predict $\Delta R/R \propto B^2$ as observed.

There is a discrepancy between our predictions and the results. The model predicts a very rapid fall in the magnetoresistance for $V < 1/\pi$; this is not seen in the experiments. This discrepancy may be due to the neglect of disorder. It is well known that there is considerable disorder in a 2D EG.⁷ The effect of this would be to smear out the rapid fall in the magnetoresistance while still preserving the low- B behavior and the dependence on a .

An alternative model for the positive magnetoresistance has been postulated by Streda and MacDonald⁸ in terms of a magnetic breakthrough of the band gap created by the periodic potential. Although the predicted magnetoresistance peaks occur at the right order of magnitude of B , we do not believe this is a satisfactory explanation for

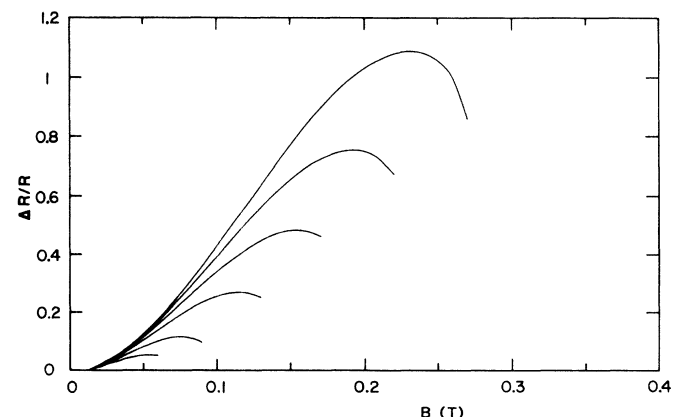


FIG. 5. Calculation of $\Delta R/R$ using Eq. (2) using $\tau = 3 \times 10^{-12}$ s, $v_F = 2.3 \times 10^5$ ms⁻¹, and $a = 300$ nm. $V_0 = 3$ (top), 2.5, 2, 1.5, 1, and 0.7 mV (bottom).

TABLE I. Nominal gate voltages and magnetic-field values for the peak in positive magnetoresistance, B_m (peak). V_0 are values of the amplitude of the electrostatic potential derived from B_m and V_0^{LL} from the quenching of the Landau levels.

V_g (V)	B_m (T)	V_0 (mV)	V_0^{LL} (mV)
0	0.11	1.2	0.73
-0.2	0.11	1.2	0.73
-0.3	0.12	1.3	0.75
-0.5	0.15	1.7	1.06
-0.6	0.18	2.0	1.34
-0.8	0.24	2.6	...
-1.0	0.31	3.4	...

two reasons. First, with the known potential disorder it is highly unlikely that superlattice minibands would occur with well-defined energy gaps. Second, Streda and MacDonald predict that the field at which the magnetoresistance peak occurs is proportional to a in contradiction to measurements made on similarly constructed samples with differing periods.

We now address the quenching of the SdH oscillations by the periodic potential. The energy of the N th Landau level E_N has been shown^{2,5} to be an oscillatory function of orbit center position, x_L ,

$$E_N(x_0) \approx (N + \frac{1}{2}) \hbar \omega_c + eV_0 J_0(2\pi R_c/a) \cos\left(\frac{2\pi x_L}{a}\right), \tag{7}$$

where $J_0(y)$ is a Bessel function and ω_c is the cyclotron frequency. This leads to a broadening of the Landau levels by an energy $\sim eV_0$ when $2R_c < a$. We anticipate that the SdH oscillations will be suppressed when this broadening is equal to the Landau-level separation $\hbar \omega_c$. We are able to deduce values for the amplitude of the potential using this condition which are also tabulated in Table I. Given the simplicity of the arguments used to derive them, the values for the potential amplitudes extracted from the data for the positive magnetoresistance peak and the SdH oscillations are consistent. We interpret this as evidence that the simple models we have used to explain our data are correct.

In conclusion, we have presented data showing how the magnetoresistance oscillations in a 2D EG subject to a one-dimensional (1D) periodic potential depend on the amplitude of that potential. The behavior at very low field may be described by a semiclassical model. We find no evidence in the experimental data currently available for the existence of miniband behavior. The dependence of the SdH oscillations is determined by the effect of the periodic potential on the density of states.

This work is supported by United Kingdom Science and Engineering Research Council (SERC). One of us (P.H.B.) thanks the Royal Society (London) and another (E.S.A.) Conselho Nacional de Desenvolvimento Científico e Tecnológico (CNPq), Brasilia, Brazil for financial support.

¹D. Weiss, K. von Klitzing, K. Ploog, and G. Weimann, *Europhys. Lett.* **8**, 179 (1989).
²R. W. Winkler, J. P. Kotthaus, and K. Ploog, *Phys. Rev. Lett.* **62**, 1177 (1989).
³E. S. Alves, P. H. Beton, M. Henini, L. Eaves, P. C. Main, O. H. Hughes, G. A. Toombs, S. P. Beaumont, and C. D. W. Wilkinson, *J. Phys. Condens. Matter* **1**, 8257 (1989).
⁴C. W. J. Beenakker, *Phys. Rev. Lett.* **62**, 2020 (1989).

⁵R. R. Gerhardt, D. Weiss, and K. von Klitzing, *Phys. Rev. Lett.* **62**, 117 (1989).
⁶P. Vasilopoulos and F. M. Peeters, *Phys. Rev. Lett.* **63**, 2120 (1989).
⁷J. A. Nixon and J. H. Davies, *Phys. Rev. B* **41**, 7929 (1990).
⁸P. Streda and A. A. MacDonald, *Phys. Rev. B* **41**, 11892 (1990).